Dynamical modelling of a genetic algorithm

E.J. Solteiro Pires, J.A. Tenreiro Machado, P.B. de Moura Oliveira

Abstract

This work addresses the signal propagation and the fractional-order dynamics during the evolution of a genetic algorithm (GA). In order to investigate the phenomena involved in the GA population evolution, the mutation is exposed to excitation perturbations during some generations and the corresponding fitness variations are evaluated. Three distinct fitness functions are used to study their influence in the GA dynamics. The input and output signals are studied revealing a fractional-order dynamic evolution, characteristic of a long-term system memory.

Keywords: Genetic algorithm; Signal processing; Dynamic; Fractional-order

1. Introduction

In the last twenty years genetic algorithms (GAs) have been applied in a plethora of fields such as in image processing, pattern recognition, speech recognition, control, system identification, optimization, planning and scheduling [1].

Fractional calculus (FC) is a natural extension of the classical mathematics. In fact, since the beginning of theory of differential and integral calculus, several mathematicians investigated the calculation of non-integer order derivatives and integrals. Nevertheless, the application of FC has been scarce until recently, but the advances in the theory of chaos motivated a renewed interest in this field.

The fundamental aspects of the FC theory are addressed in [2–5]. In what concerns the FC application we can mention research on viscoelasticity/damping, chaos/fractals, biology, electronics, signal processing, diffusion and wave propagation, percolation, modelling, control and irreversibility [6–19,23].

Bearing these ideas in mind, this paper analyzes the system signal evolution and the fractional-order dynamics in the population of a GA-based optimization. The article is organized as follows. Section 2 introduces the problem and the GA method for its resolution. Based on this formulation, Section 3 presents the results for several simulations involving different working conditions and studies the resultant dynamic phenomena. Section 4 present the same simulation with others fitness functions and

compare the results. Finally, Section 5 outlines the main conclusions.

2. The optimization GA

This section presents the optimization GA used in the study of the dynamic system. To investigate the influence of the fitness function in the GA, are used three simple functions $\{f_A; f_B; f_C\}$, each at a time,
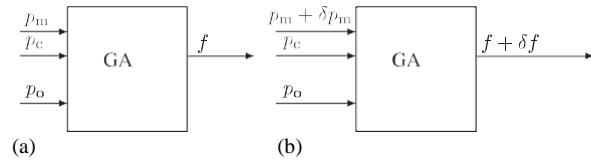

(a)   (b)

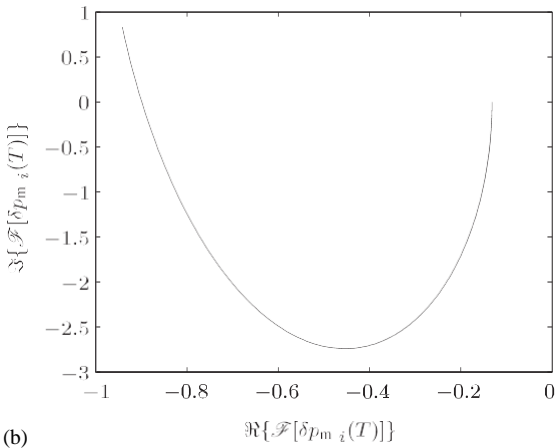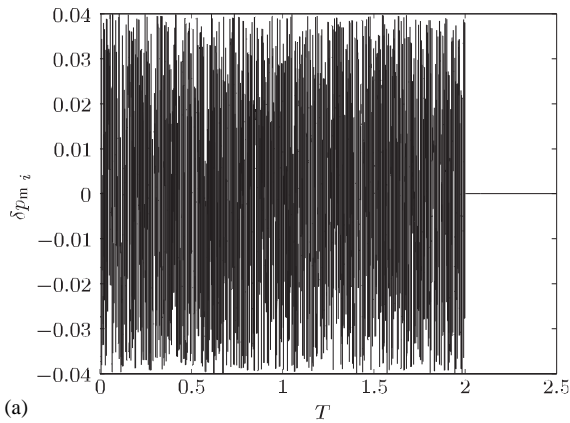Fig. 1. System dynamics. (a) Initial system, (b) perturbed system.

given by the expressions

$$f_A(b) = 1 + |b - 41|, \qquad (1a)$$
$$f_B(b) = 1 + |b - 41|^2, \qquad (1b)$$
$$f_C(b) = 2 - \text{sinc}(b - 41), \qquad (1c)$$
$$b = \{b_1, b_2, b_3, \ldots, b_l\}. \qquad (2)$$

The objective consists on minimizing each function that depends on the parameter $b \in [-50000; 50000]$. In the experiments, involving the three test functions, it is adopted a binary Gray code, with the string length of $l = 24$ bits to represent the solutions of the population (2) while having an identical initial population. The same applies for the genetic parameters, namely (i) a 50-population GA, (ii) an execution during 200 generations, (iii) a rank selection having simple crossover and mutation with probabilities $p_c = 0.8$ and $p_m = 0.05$, respectively. Moreover, the best solution of each generation is always passed to the next generation. The
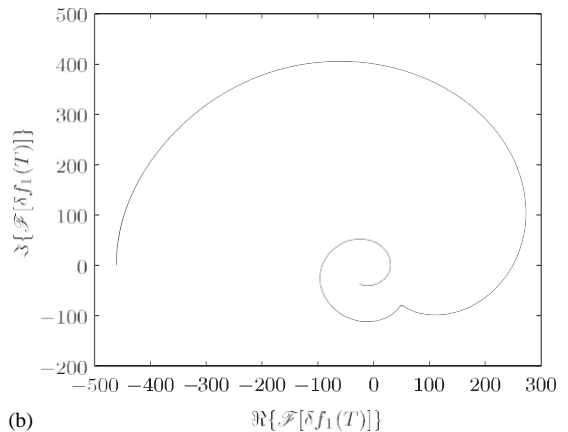

(a)

(b)

Fig. 2. Input signal dp_m perturbation over $T_{exc} = 2$ generations with seed $i = 1$ ($Dp = 0.04$, fitness f_A). (a) Generation domain, (b) polar diagram.

(a)

(b)
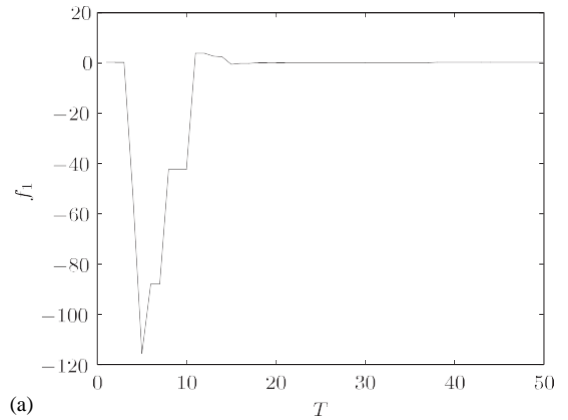
Fig. 3. Output variation $df(\delta T)$ for the input excitation over $T_{exc} = 2$ generations with seed $i = 1$ ($Dp = 0.04$, fitness f_A). (a) Generation domain, (b) polar diagram.

influence of several factors can be analyzed in order to study the dynamics of the GA, particularly the probabilities. This influence can be distinct according to the type of selection, elitism, fitness function and string length used in the GA. In this work,
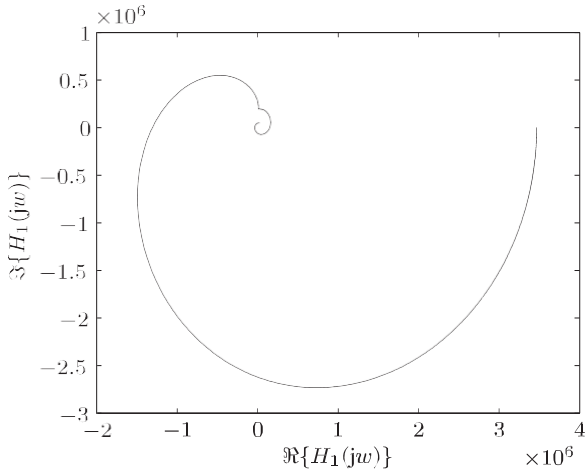

Fig. 4. Transfer function $H_1(jw)$ using seed $i = 1$ ($T_{exc} = 2$, $\Delta p = 0.04$, fitness f_A).

across each test function experiment, it is changed only the initial seed of the mutation probability noise that is added to p_m.

3. Evolution, signal propagation and fractional-order dynamics

This section studies the dynamical phenomena involved in the signal propagation within the GA population. In this perspective, small amplitude perturbations are superimposed over biasing signals of the GA system and its influence upon the population fitness is evaluated. The experiments reveal a fractional-order dynamics capable of being described by systems theory tools.

3.1. Introduction to fractional calculus

Since the foundation of the differential calculus the generalization of the concept of derivative and integral to a non-integer order a has been the subject of distinct approaches. Due to this reason there are several alternative definitions of fractional
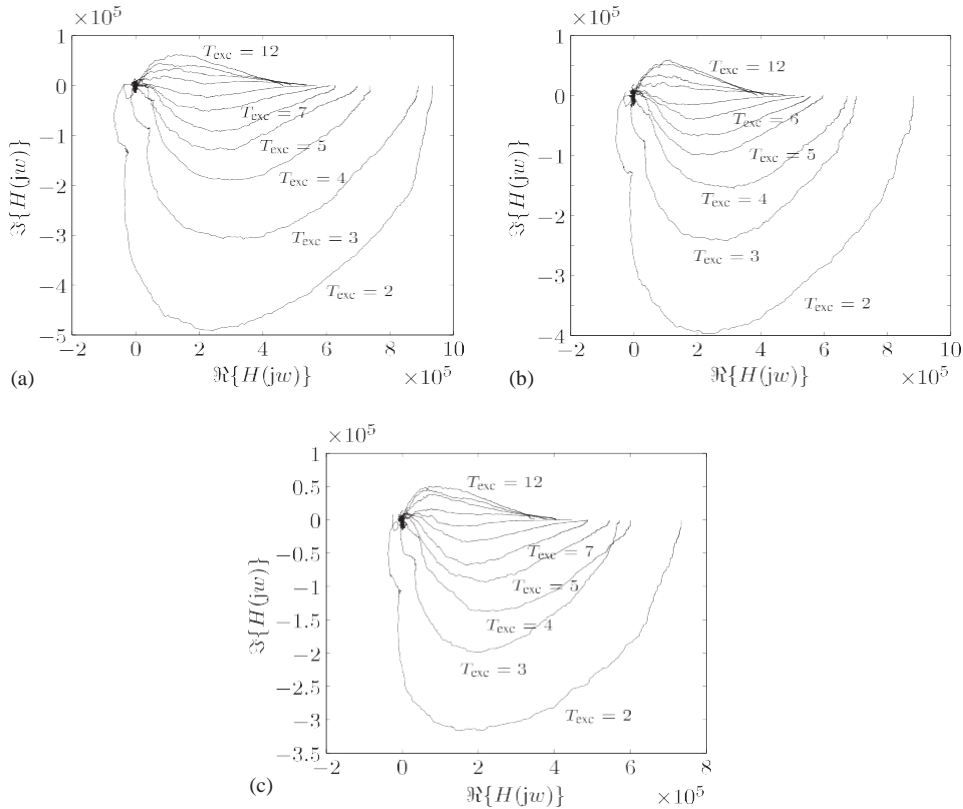

Fig. 5. Polar diagrams of $H_A(jw)$ for $\Delta p = \{0.03; 0.04; 0.05\}$, $n = 1701$. (a) Polar diagram with $\Delta p = 0.03$, (b) polar diagram with $\Delta p = 0.04$, (c) polar diagram with $\Delta p = 0.05$.

derivatives. For example, the Laplace definition of a derivative of fractional order $a \in \mathbb{C}$ of the signal $x(t)$, $D^{a}[x(t)]$, is a 'direct' generalization of the classic integer-order scheme yielding to Eq. (3). This means that frequency-based analysis methods have a straightforward adaptation (for zero initial conditions):

$$\mathscr{L}\{D^{a}[x(t)]\} = s^{a}X(s). \qquad (3)$$

An alternative approach, based on the concept of fractional differential, is the Grünwald–Letnikov definition given by Eq. (4)

$$D^{a}[x(t)] = \lim_{h \to 0} \left[\frac{1}{h^{a}} \sum_{k=0}^{+\infty} (-1)^{k} \right.$$
$$\left. \times \frac{\Gamma(\alpha + 1)}{\Gamma(k+1)(\alpha - k + 1)} x(t - kh) \right]. \qquad (4)$$
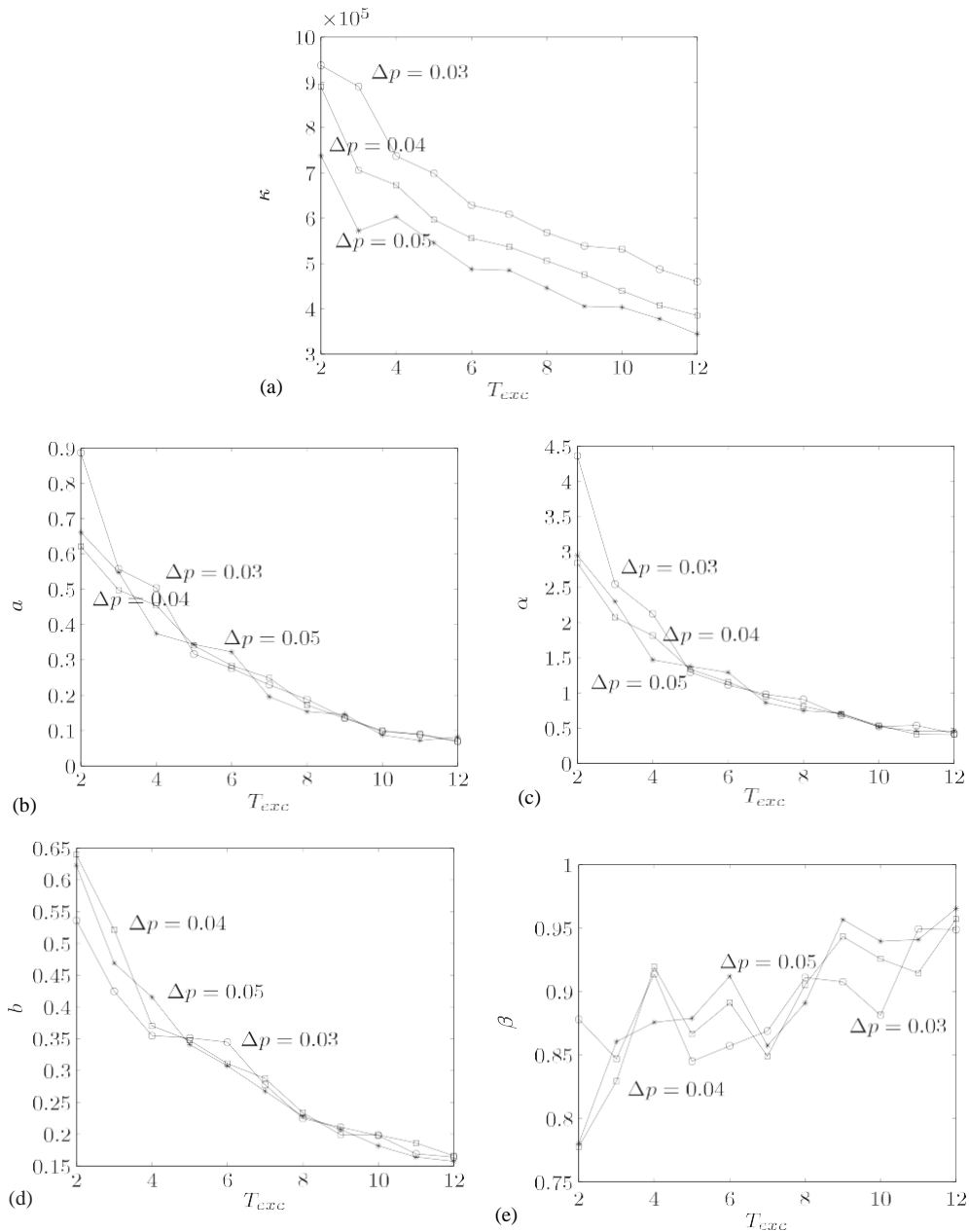
(a)

(b)

(c)

(d)

(e)

Fig. 6. Estimated gain, poles and fractional-orders vs. T_{exc} for fitness f_A. (a) Gain k vs. T_{exc}, (b) pole a vs. T_{exc}, (c) pole fractional-order a vs. T_{exc}, (d) pole b vs. T_{exc}, (e) pole fractional-order b vs. T_{exc}.

An important property revealed by this equation is that while an integer-order derivative implies just a finite series, the fractional-order derivative requires an infinite number of terms. This means that integer derivatives are 'local' operators in opposition with fractional derivatives that have, implicitly, a 'memory' of all past events.

The characteristics revealed by fractional-order models make this mathematical tool well suited to describe phenomena such as irreversibility and chaos because of its inherent memory property. In this line of thought, the propagation of perturbations and the appearance of long-term dynamic phenomena in a population of individuals subjected to an evolutionary process seem to be a case where FC tools fit adequately.

3.2. The GA dynamics

In this section the GA system is stimulated by perturbing the mutation probability, p_m, through a white noise signal, dp_m, and the corresponding

Table 1
Parameters of g_i, $i ¼ f1; 2g$ for $fk; a; a; b; bg$ approximation of f_A optimization function

Dp	k		a		a		b		b	
	$g_1 ð10^5 Þ$	g_2	g_1	g_2	g_1	g_2	g_1	g_2	g_1	g_2
0.03	10.0	−0.40	2.90	−1.40	10.86	0.99	0.93	−0.67	0.83	0.04
0.04	10.0	−0.44	2.12	−1.26	7.42	−1.11	1.14	−0.76	0.75	0.09
0.05	9.7	−0.39	2.50	−1.31	7.23	−1.10	1.16	−0.79	0.75	0.10
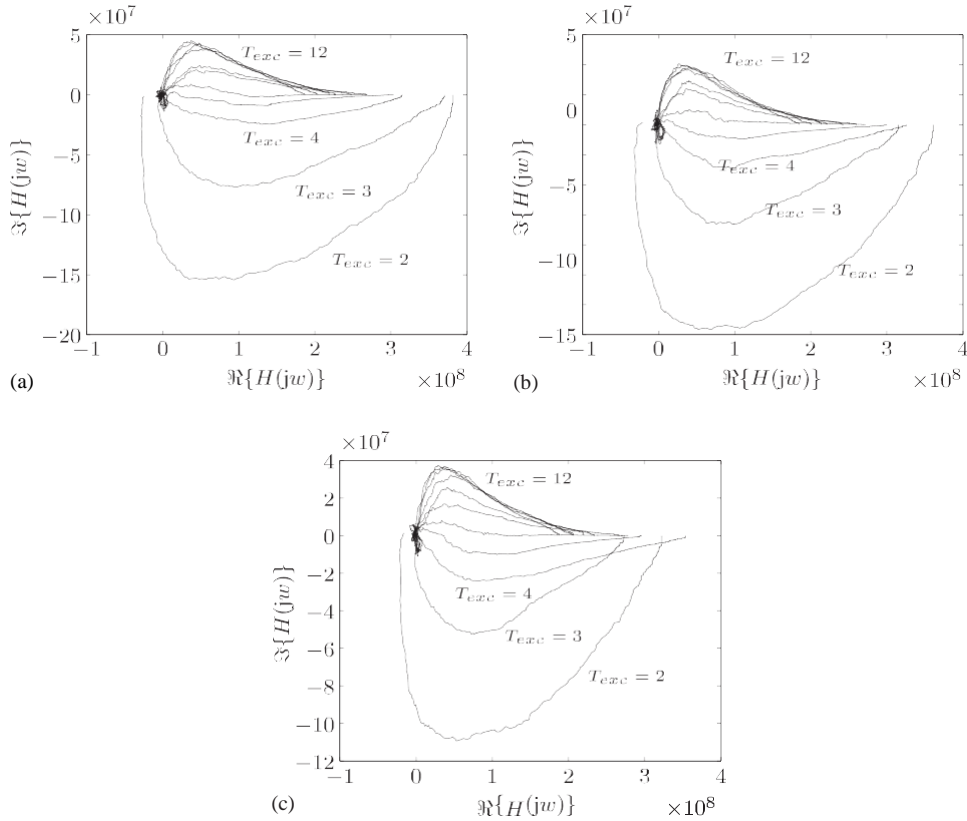
Fig. 7. Polar diagrams of $H_B ðjwÞ$ for $Dp ¼ f0:03; 0:04; 0:05g$, $n ¼ 1701$. (a) Polar diagram with $Dp ¼ 0:03$, (b) polar diagram with $Dp ¼ 0:04$, (c) polar diagram with $Dp ¼ 0:05$.
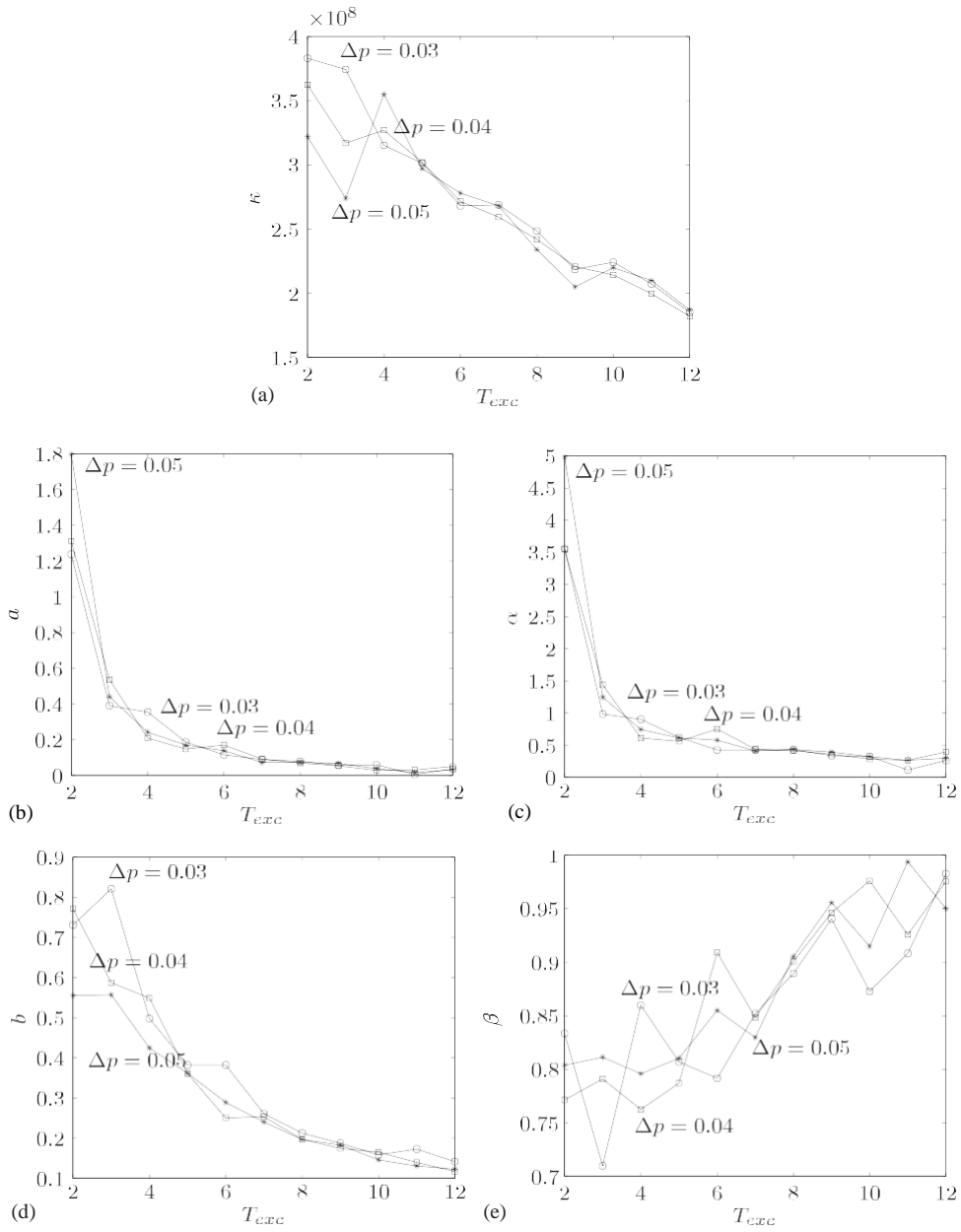
Fig. 8. Estimated gain, poles and fractional-orders vs. T_{exc} for fitness f_B. (a) Gain $\mathtt{k}$ vs. T_{exc}, (b) pole a vs. T_{exc}, (c) pole fractional-order $\mathtt{a}$ vs. T_{exc}, (d) pole b vs. T_{exc}, (e) pole fractional-order $\mathtt{b}$ vs. T_{exc}.

Table 2
Parameters of g_i, i ¼ f1; 2g for f$\mathtt{k}$; a; $\mathtt{a}$; b; $\mathtt{b}$g approximation of f_B optimization function

Dp	$\mathtt{k}$		a		$\mathtt{a}$		b		$\mathtt{b}$	
	g_1 ð10^8Þ	g_2	g_1	g_2	g_1	g_2	g_1	g_2	g_1	g_2
0.03	6.0	−0.40	6.39	−2.26	6.87	−1.44	2.02	−1.05	0.70	0.11
0.04	5.0	−0.38	4.66	−2.03	5.65	−1.25	1.93	−1.09	0.66	0.15
0.05	4.0	−0.30	6.83	−2.27	7.39	−1.40	1.42	−0.95	0.70	0.12

population fitness modification δf is evaluated, see Fig. 1. The crossover and other probability signals used, p_c and p_o, remain unchanged. Therefore, the variation of the mutation probability and the resulting fitness modification on the GA population, during the evolution, can be viewed as the system inputs and output signals varying during the successive generations. This analysis is evaluated using several experiments with different seeds for a small amplitude white noise perturbation signal. All the other seeds remain unchanged.

In this perspective, a white noise signal $\delta p_m(T)$ is added to the mutation probability p_m of the strings during a time period T_{exc} and the new mutation probability p_n is calculated by Eq. (5) where Z is the white noise signal with maximum amplitude $\pm\Delta p$

$$p_n = \begin{cases} 0 & \text{if } p_m + \eta(\Delta p) < 0, \\ 1 & \text{if } p_m + \eta(\Delta p) > 1, \\ p_m + \eta(\Delta p) & \text{otherwise.} \end{cases} \qquad (5)$$

Consequently, the input signal, at generation T, is the difference between the two cases, that is $\delta p_m(T) = p_n(T) - p_m(T)$. On the other hand, the output signal is the difference in the population fitness with and without noise, that is $\delta f(T) = f_n(T) - f(T)$.

Fig. 2 shows the input signal $\delta p_m(T)$, with seed $i = 1$, in the generation domain and the corresponding polar diagram, for f_A, $\Delta p = 0.04$ and $T_{exc} = 2$, where $\mathcal{F}[\delta p_m(T)]$ represents the Fourier transform of the signal perturbation. Fig. 3 shows the corresponding output signal variation $\delta f(T)$.

Once having de Fourier description of the input and output signals it is possible to calculate the corresponding transfer function (6) for seed i

$$H_i(jw) = \frac{\mathcal{F}\{\delta f_i(T)\}}{\mathcal{F}\{\delta p_{m_i}(T)\}}, \quad i = \{1,\dots,n\}. \qquad (6)$$

The transfer function $H_i(jw)$, with seed $i = 1$, between the input and output signals, is depicted in Fig. 4.

After repeating for all seeds a 'representative' transfer function is obtained by using the median of the statistical sample [20,21] of n experiments.

3.3. Transfer function identification

In this section the median of the numerical system transfer function, Fig. 5, is approximated by analytical expressions with gain $k \in \mathbb{R}$ and two

poles $(a, b) \in \mathbb{R}$ of fractional orders $(a, b) \in \mathbb{R}$, respectively, given by Eq. (7) where $l = A$ for function f_A

$$G_l(jw) = \frac{\kappa}{[(jw/a) + 1]^\alpha[(-jw/b)^\beta + 1]}. \qquad (7)$$

Note that expression (7) is a transfer function adopting left and right half-plane poles a and b, respectively.

In order to estimate the transfer function parameters, an identification GA adopting a real string is executed with the representation $\{k; a; b; a; b\}$. The identification GA is executed during $T_{ide} = 600$ generations with a 100 strings population. It is used

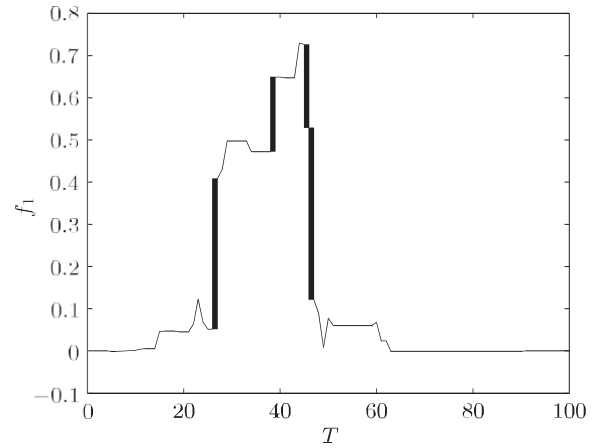Fig. 9. Output variation $\delta f(T)$ for fitness f_C and for the input excitation over $T_{exc} = 2$ generations with seed $i = 1$ ($\Delta p = 0.04$).
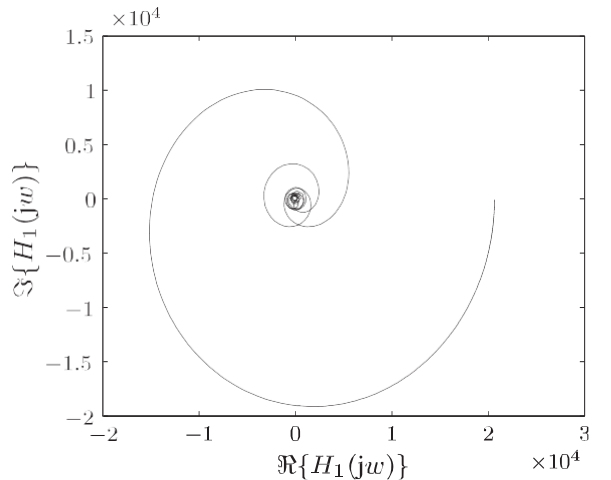
Fig. 10. Transfer function $H_1(jw)$ for fitness f_C and using seed $i = 1$ ($T_{exc} = 2$, $\Delta p = 0.04$).

the simulated binary crossover [22] and, when one mutation occurs, the corresponding value $\{x_1; \ldots; x_5\} - \{k; a; b; a; b\}$ is changed according with the equations:

$$x_{i+1} = 10^{u_i} x_i, \tag{8a}$$

$$u_i \sim U[-\varepsilon_i, +\varepsilon_i], \tag{8b}$$

where u_i is a random number generated through the uniform probability distribution U and e_i is fixed according with the range of estimation.

The fitness function f_{ide} measures the distance between the median $H(jw_k)$ and $G(jw_k)$:

$$f_{ide} = \sum_{k=1}^{nf} \|H(jw_k) - G(jw_k)\|, \tag{9}$$

where H represents the median of the n transfer functions resulting for each different seed, nf is the total number of sampling points and w_k, $k = \{1; \ldots; nf\}$ is the corresponding vector of frequencies.

Since the optimization GA has a stochastic dynamics, each execution of the GA, with a different noise seed, leads to a different transfer function. Consequently, in order to obtain a numerical convergence [20] are performed $n = 1701$ perturbation experiments, for each optimization function, with different seeds for the white noise signal, $dp_m(T)$ (all the other seeds for p_m, p_c and selection remains unchanged). So, the transfer function of the optimization GA dynamics is evaluated by computing the Fourier transform (FT) for each pair of input and output signals. After that, the medians of the transfer functions calculated previously (i.e., for each real and imaginary part and for each frequency) are taken as the final part of the numerical transfer function $H(jw)$ (see Fig. 5).

For evaluating the influence of the excitation period T_{exc} several simulations are performed ranging from $T_{exc} = 2$ to $T_{exc} = 12$ generations. The relation between the transfer function parameters and T_{exc} are shown in Fig. 6.
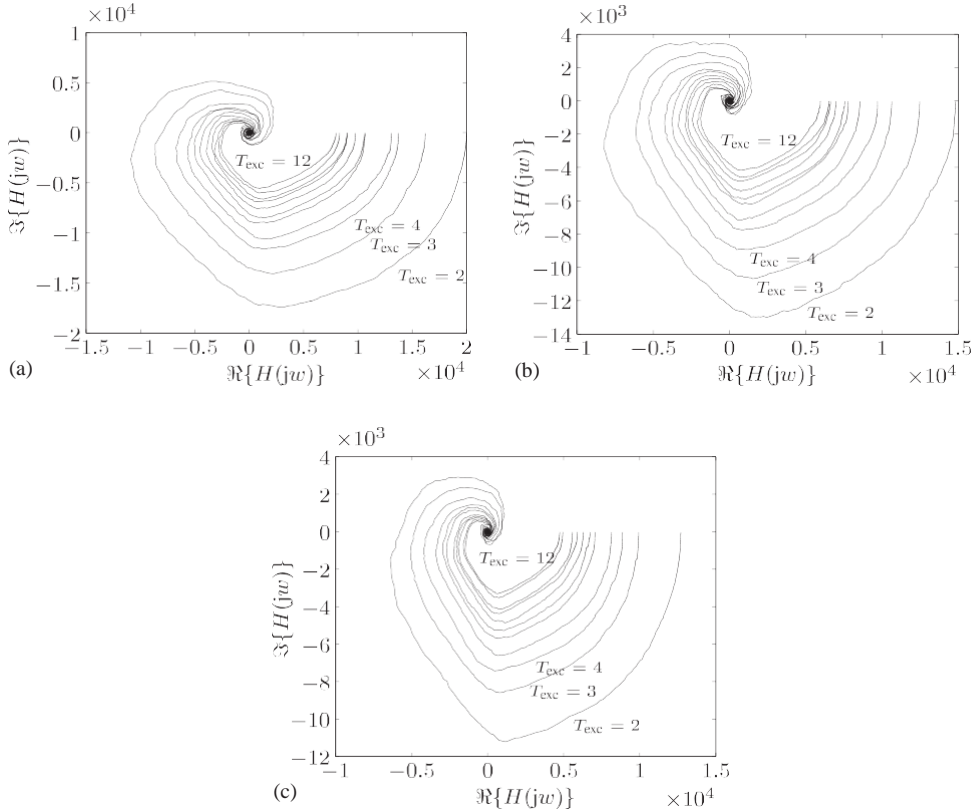

Fig. 11. Polar diagrams of $H(jw)$ for fitness $f_c(b)$ and $Dp = \{0:03; 0:04; 0:05\}$, $n = 1701$. (a) Polar diagram with $Dp = 0:03$, (b) polar diagram with $Dp = 0:04$, (c) polar diagram with $Dp = 0:05$.

The charts of {k; *a*; *b*; a; bg can be approximated through Eq. (10) leading to the parameters of Table 1.

$$\{\kappa, a, \alpha, b, \beta\} \simeq \gamma_1 (T_{\mathrm{exc}})^{\gamma_2}. \tag{10}$$

These results reveal that the transfer function parameters {k; *a*; a; *b*; bg vary with a power law vs. the excitation time T_{exc}. Moreover, all the parameters have a strong dependence with T_{exc} on the transfer function. Furthermore, k varies with D*p* and p_{m} while f*a*; a; *b*; bg have a low dependence with D*p* and p_{m}.

By enabling the zero/pole order to vary freely, we get non-integer values for a and b. Alternatively, the adoption of an integer-order transfer function would lead to a larger number of zero/poles to get the same quality in the analytical fitting to the numerical values. The 'requirement' of fractional-order models, in opposition with the classical case of integer models, is a well-known discussion and even nowadays final conclusions are not clear since it is always possible to approximate a fractional frequency response through an integer one as long as we make use of a larger number of zeros and
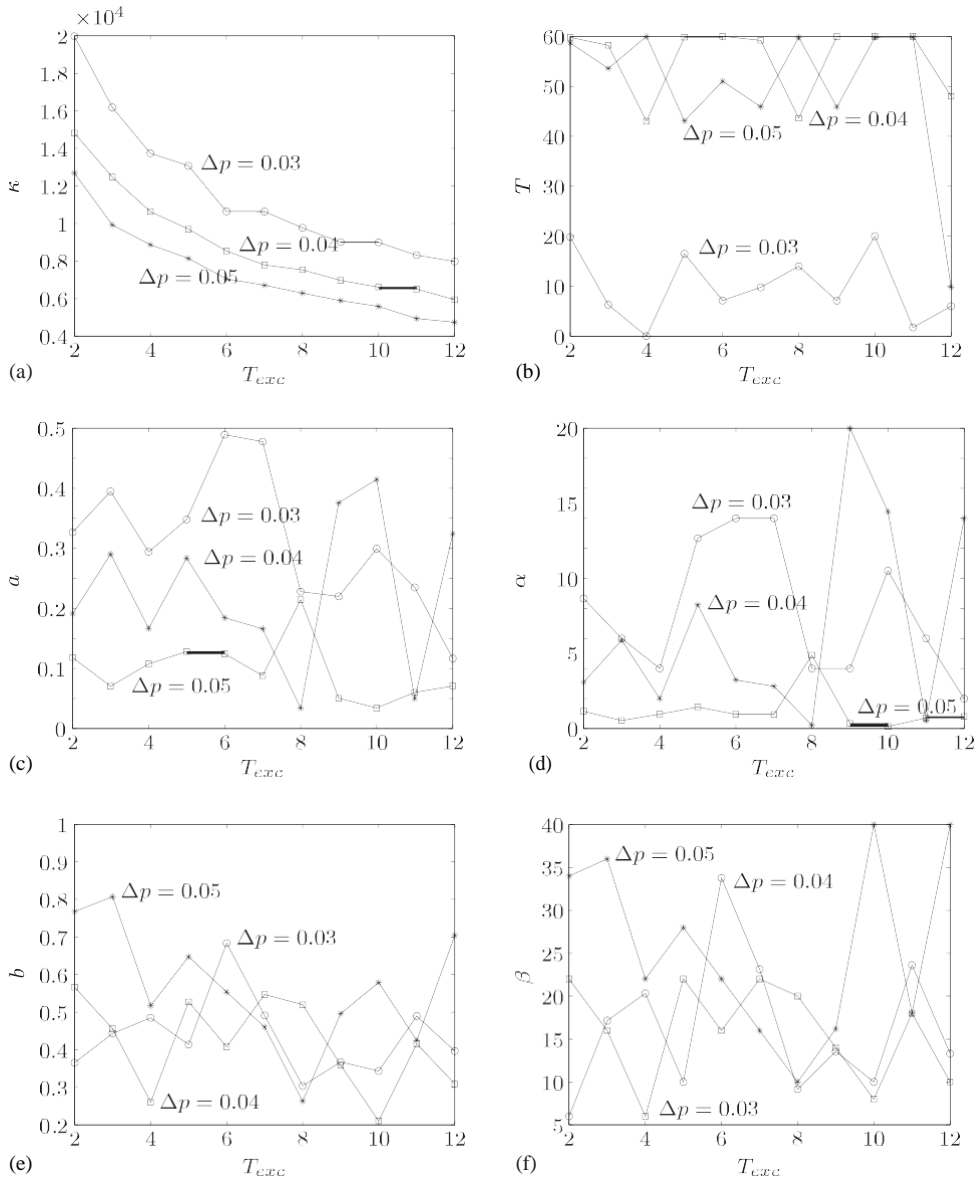
Fig. 12. Estimated parameters vs. T_{exc} for fitness f_C. (a) Gain k vs. T_{exc}, (b) delay T vs. T_{exc}, (c) pole *a* vs. T_{exc}, (d) pole fractional-order a vs. T_{exc}, (e) pole *b* vs. T_{exc}, (f) pole fractional-order b vs. T_{exc}.

poles. Nevertheless, the present experiments constitute a complementary point of view towards the adoption of FC.

4. Experiments with the fitness functions f_B and f_C

In this section is presented the polar diagram and the correspondent parameters approximation when is used the f_B and f_C optimization functions. The experiments are carried out in the same conditions as the previous section.

The polar diagrams obtained for f_B can be seen in Fig. 7. Adopting again the transfer function (7), with l ¼ B, it yields the estimated parameters fk; a; a; b; bg depicted in Fig. 8. These parameters can be approximated also through the power expressions (10) leading to the results shown in Table 2. Function f_B reveals a behavior with similarities to the previous case, with exception of the gain k that has a small variation with Dp.

The study of the fitness function f_C follows an identical strategy. Nevertheless, it results a different type of output and transfer function as can be seen in Figs. 9 and 10. The output is less sensitive and responds only after a delay of several generations. Consequently, this optimization GA leads to a different polar diagrams for HðjwÞ (see Fig. 11). In this case the median HðjwÞ can be approximated by

$$G_C(jw) = \frac{\kappa e^{-jwT}}{[(jw/a) + 1]^{\alpha}[(jw/b) + 1]^{\beta}} \qquad (11)$$

leading to a minimum phase system in contrast to the previous cases.

In this simulation only k (Fig. 12) follows clearly Eq. (10), resulting the estimated values depicted in Table 3. The other parameters reveal a kind of noisy behavior and no clear trendlines emerge. Nevertheless, in order to easy comparisons it was decided to maintain the parameters estimation through (10) leading to exponents g_2 close to zero.

5. Conclusions

This paper analyzed the signal propagation and the dynamic phenomena involved in the time evolution of a population of individuals. The study was established on the basis of a simple GA optimization using three different functions. While the study of GA schemes has been extensively studied, the influence of perturbation signals over the operating conditions is not well known.

From the results can be concluded that the optimization functions and the time duration of perturbation have a strong influence upon the behavior of the GA while the value adopted for the mutation probability seems to be less significant.

Bearing these ideas in mind, a FC calculus perspective was introduced in order to develop approximating transfer functions analytically simple yet meaningful. It was shown that fractional-order models capture phenomena and properties that classical integer-order sometimes overlook due to the approximation requirement for the introduction of a large number of parameters that makes things unclear.

Table 3
Parameters of g_i, i ¼ f1; 2g for fk; T; a; a; b; bg approximation of f_C optimization function

Dp	k				T		
	g_1		g_2		g_1		g_2
(a) k; T parameters vs. Dp							
0.03	28328		−0.51		0.34		1.17
0.04	21467		−0.51		57.22		0.02
0.05	18418		−0.53		87.80		−0.36

(b) a; a; b; b parameters vs. Dp								
Dp	a		a		b		b	
	g_1	g_2	g_1	g_2	g_1	g_2	g_1	g_2
0.03	0.58	−0.38	11.71	−0.32	0.45	−0.04	9.65	0.23
0.04	0.16	−0.35	1.50	−0.35	0.61	−0.23	19.72	−0.16
0.05	0.25	−0.18	34.51	−0.21	0.88	−0.27	3.09	−0.08

Acknowledgment

References

[1] T. Ba̋ck, U. Hammel, H.-P. Schwefel, Evolutionary compu- tation: comments on the history and current state, IEEE Trans. Evolutionary Comput. 1 (1) (1997) 3–17.

[2] B. Ross, Fractional Calculus and its Applications, Lecture Notes in Mathematics, vol. 457, Springer, Berlin, 1974.

[3] K.S. Miller, B. Ross, An Introduction to the Fractional Calculus and Fractional Differential Equations, Wiley, New York, 1993.

[4] K.B. Oldham, J. Spanier, The Fractional Calculus: Theory and Application of Differentiation and Integration to Arbitrary Order, Academic Press, New York, 1974.

[5] S.G. Samko, A.A. Kilbas, O.I. Marichev, Fractional Integrals and Derivatives: Theory and Applications, Gordon and Breach Science Publishers, New York, 1993.

[6] A. Gement, On fractional differentials, Proc. Philos. Mag. 25 (1938) 540–549.

[7] A. Oustaloup, La Commande CRONE: Commande Ro-buste d'Ordre Non Intier, Hermes, 1991.

[8] A. Oustaloup, La De´rivation Non Entier: The´orie, Synthe`se et Applications, Editions Hermes, 1995.

[9] C.G. Koh, J.M. Kelly, Application of fractional derivatives to seismic analysis of base-isolated models, Earthquake Eng. Struct. Dyn. 19 (1990) 229–241.

[10] J.A. Tenreiro Machado, Analysis and design of fractional-order digital control systems, J. System Anal.—Modelling-Simulation 27 (1997) 107–122.

[11] J.A. Tenreiro Machado, System modeling and control through fractional-order algorithms, FCAA—J. Fractional Calculus Appl. Anal. 4 (2001) 47–66.

[12] I. Podlubny, Fractional Differential Equations, Academic Press, San Diego, 1999.

[13] B.M. Vinagre, I. Petras, I. Podlubny, Y.Q. Chen, Using fractional order adjustment rules and fractional order reference models in model-reference adaptive control, Non-linear Dyn. 1–4 (29) (2002) 269–279.

[14] P.J. Torvik, R.L. Bagley, On the appearance of the fractional derivative in the behaviour of real materials, ASME J. Appl. Mech. 51 (1984) 294–298.

[15] O.P. Agrawal, Solution for a fractional diffusion-wave equation in a bounded domain, Nonlinear Dyn. 29 (1–4) (2002) 145–155.

[16] S. Westerlund, Dead Matter Has Memory! Causal Consult-ing, Kalmar, Sweden, 2002.

[17] T.J. Anastasio, The fractional-order dynamics of brainstem vestibulo-oculomotor neurons, Biol. Cybern. 72 (1994) 69–74.

[18] Y. Chen, K.L. Moore, Discretization schemes for fractional-order differentiators and integrators, IEEE Trans. Circuits Systems 49 (3) (2002) 363–367.

[19] A.L. Me´ haute´ , Fractal Geometries: Theory and Applica- tions, Penton Press, Golden, Columbia, 1991.

[20] J.A. Tenreiro Machado, A.M.S.F. Galhano, A statistical perspective to the Fourier analysis of mechanical manip-ulators, J. Systems Anal.—Modelling-Simulation 33 (1998) 373–384.

[21] L. Figueiredo, J.A. Tenreiro Machado, J.R. Ferreira, Dynamical analysis of freeway traffic, IEEE Trans. Intell. Transp. Systems 5 (4) (2004) 259–266.

[22] K. Deb, Multi-Objective Optimization Using Evolutionary Algorithms, Wiley, New York, 2001.

[23] E.J. Solteiro Pires, J.A. Tenreiro Machado, P.B. de Moura Oliveira, Fractional order dynamics in a GA planner, Signal Process. 83 (11) (2003) 2377–2386.